# Microring Weight Banks

Alexander N. Tait, Allie X. Wu, Thomas Ferreira de Lima, Ellen Zhou, Bhavin J. Shastri, *Member, IEEE*, Mitchell A. Nahmias, and Paul R. Prucnal, *Fellow, IEEE*

***Abstract*—Microring weight banks could enable novel signal processing approaches in silicon photonics. We analyze factors limiting channel count in microring weight banks, which are central to analog wavelength-division multiplexed processing networks in silicon. We find that microring weight banks require a fundamentally different analysis compared to other wavelength-division multiplexing circuits (e.g., demultiplexers). By introducing a quantitative description of independent weighting, we establish performance tradeoffs between channel count and power penalty. This performance is significantly affected by coherent multiresonator interactions through bus waveguides. We experimentally demonstrate these effects in a fabricated device. Analysis relies on the development of a novel simulation technique combining parametric**

channel has not been performed. WG circuits of similar ge-

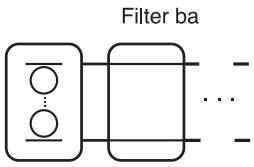
Filter ba

Fig. 4(b) shows that bus tuning significantly affects the dip between filters, whose depth ranges from ~ 2.7 dB to ~ 25.0 dB relative to peak transmission. The steepness of rolloff regions are also slightly affected. The measurements closely match corresponding simulations in which the effective bus phases were parameterized and swept uniformly, shown in Fig. 4(c). This verifies that the parametric simulator can make accurate predictions about weight banks in the dense channel regime. While the device layout is symmetric, the asymmetry observable in the spectra of Fig. 4(b) and (c) can be explained by the fact that inputs encounter the MRRs in a particular order.

From an intuitive standpoint, it seems that this coherent effect that depends on bus phase could have a significant impact on channel density. If the goal is to be able to set the weight/transmission of neighboring WDM channels independently, then it would be disadvantageous to have the responses blur into a single peak like the red traces in Fig. 4(b) and (c). On the other hand, it may be possible to take advantage of the deep isolation between peaks represented by the blue traces. Bus tuning elements could prove useful in large scale MRR weight banks because they provide full control over multi-MRR effects, which may be otherwise difficult to control in the presence of fabrication variance and thermal cross-talk. In Section V, we will quantify the degree to which weights can be set independently and use the simulator to study how this metric is affected by channel spacing and MRR interaction. An approach for efficient simulation of tunable MRR devices with multiple coherent paths is now discussed in more detail.

## IV. Parameterized Simulator

Parameterized modeling is a powerful tool for engineering analysis, particularly for tunable systems. While a numerical simulation can predict the response of a particular device in a particular state, a parameterized model is a function of free parameters or can be thought of as a representation of all the possible states of a particular device. Combined with different search and optimization functions, parameterized models are at the heart of problems such as finding a state that reproduces an observed response (e.g. measurement fitting), finding a state that gives a desired response (e.g. optimization, feedforward

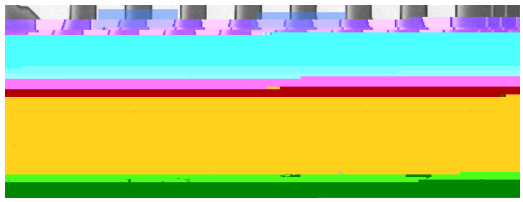

W

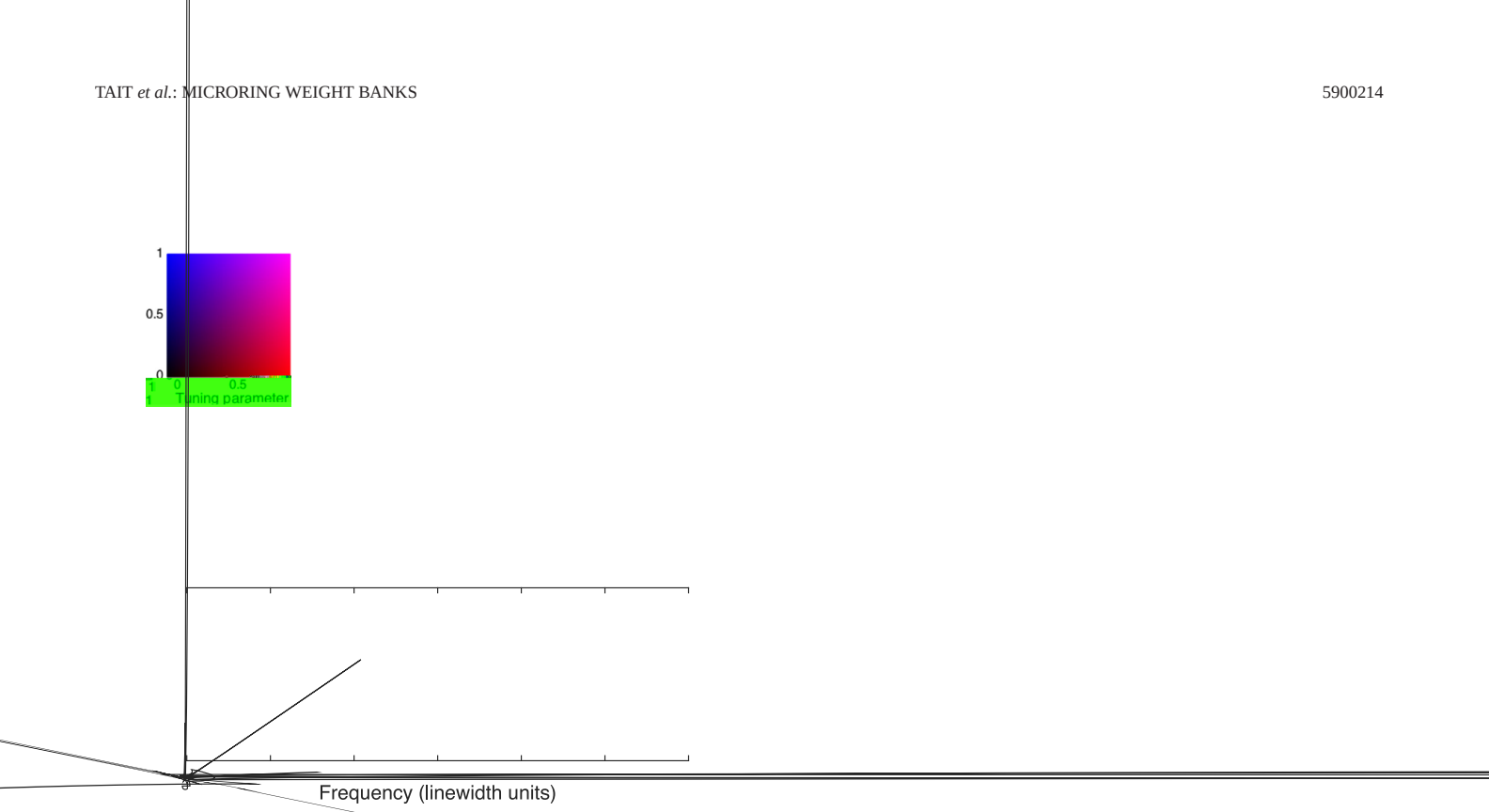
1
0.5
0
1
0
0.5
1
Tuning parameter
Frequency (linewidth units)

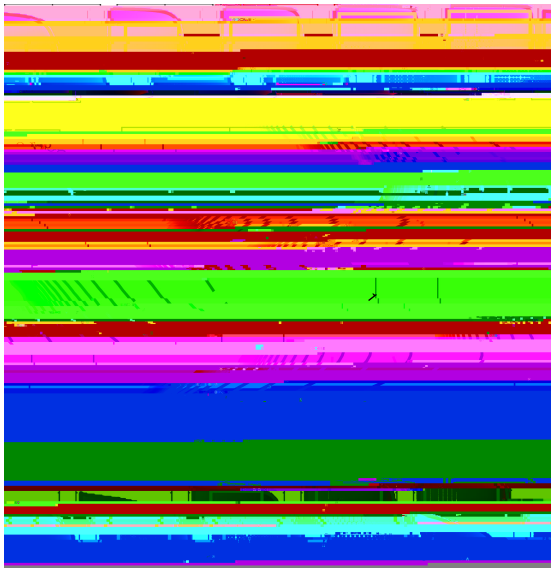

communications in silicon photonics [50], [51] and therefore can be expected to improve.

The footprint of the filters needed for a network can be estimated from the channel count and resonator size. Supposing we use the resonator from [44] (channel count = 108), then the approximate footprint of a single filter bank in this case is $108 \cdot 5\ \mu\text{m} \cdot 5\ \mu\text{m} = 2700\ \mu\text{m}^2$. The corresponding $N$-to-$N$ network footprint is $108 \cdot 2700 = 0.29\ \text{mm}^2$. We have made the simplifying assumptions that every connection has a dedicated tunable MRR filter, these filters are all critically coupled to the bus WG, and that they are single-pole (i.e. single-MRR).

## VI. Discussion

While the rigorous numeric result for channel number is im-

transfer matrix $A_{\mathrm{MRR}}$ which relates the left-hand side inputs (1:IN and 2:DROP) to the right-hand side outputs (3:THRU and 4:ADD) as such:

$$\begin{bmatrix} a_1 & b_1 & a_2 & b_2 \end{bmatrix}^T = A_{\mathrm{MRR}} \begin{bmatrix} b_3 & a_3 & b_4 & a_4 \end{bmatrix}^T$$

where $a_i$ and $b_i$ represent signals coming respectively into and out of port $i$ as in ref. [36]. This is useful because the scattering transfer matrix multiple MRRs is the product of the individual scattering transfer matrices. Another possible representation of a 4-port coupler is the scattering matrix $S_{\mathrm{MRR}}$, which gives the relationship between outcoming signals and incoming signals to all ports:

$$\begin{bmatrix} b_1 & b_2 & b_3 & b_4 \end{bmatrix}^T = S_{\mathrm{MRR}} \begin{bmatrix} a_1 & a_2 & a_3 & a_4 \end{bmatrix}^T.$$

The relationship between $S_{\mathrm{MRR}}$ and $A_{\mathrm{MRR}}$ can be easily derived and is explicitly shown in ref. [36]. The S matrix for a single MRR using a type-3 coupler (see Fig. 3(b)) design described above should have the form:

$$S_{\mathrm{MRR}} = \begin{bmatrix} 0 & D_1 & T_1 & 0 \\ D_1 & 0 & 0 & T_2 \\ T_1 & 0 & 0 & D_2 \\ 0 & T_2 & D_2 & 0 \end{bmatrix} \tag{15}$$

where we introduced the parameters $D_{1,2}$ and $T_{1,2}$ to highlight the symmetry of the system: e.g. if the input is in port 1, the transmission ($S_{31}$) and drop ($S_{21}$) coefficients are $T_1$ and $D_1$, respectively. Note that we have ignored here backscattering terms ($S_{11} = S_{41} = 0$). The asymmetry between $T_1$ and $T_2$ is explained by the different coupling coefficients $K_1$ and $K_2$ and that of $D_1$ and $D_2$ is explained by the possible different path lengths of each arm of the microring. These distinctions will soon be mathematically clear. This matrix was explicitly calculated in ref. [55]. However, the analysis of a weight bank filter will require an intuitive way of expressing each term $T_j$ and $D_j$, because multiple rings will interfere with each other in interesting ways. First, we define a set of helpful variables: the round-trip amplitude loss of the microring cavity as $G \equiv a^2 (1 - K_1)(1 - K_2) \exp(-\alpha L)$, where $L = L_1 + L_2$ is the cavity length (see Fig. 3(a)); and the cavity-resonance amplification factor

every ring, which explains the summing term $\sum_{m=1}^{m=n} D_{1,\mathrm{L}(m)}$. Each interfering term at the drop port of A, however, is amplified by the resonant feedback of pairs of rings formed by A and another ring to the *right* of A. Equation (16) is more complicated to understand, but it was derived and analytically verified by symbolic calculation of the $S_3 1$ and $S_2 1$ originating from cascaded scattering transfer matrix multiplication employed in Section II-B1.

The interest of the analytical expressions (14) and (15) is that it allows for smart approximation of scattering terms for a great number of MRRs ($n$ 1): one could, for example, neglect all resonant feedback and only consider microring resonances ($F_{AB} = FBC =$ = 1), or one could neglect resonant feedback of more than three rings ($F_{AC} = FBD =$ = 1), making the analysis more tractable. We hope that these analytical expressions will help optimize the design of large filter banks taking into account coherent interference.

## ACKNOWLEDGMENT

Fabrication support was provided via the Natural Sciences and Engineering Research Council of Canada Silicon Electronic-Photonic Integrated Circuits Program. Devices were fabricated by Richard Bojko at the University of Washington Washington Nanofabrication Facility, part of the NSF National Nanotechnology Infrastructure Network.

## REFERENCES

[1] G. T. Reed, G. Mashanovich, F. Y. Gardes, and D. J. Thomson, "Silicon optical modulators," *Nature Photonics*, vol. 4, no. 8, pp. 518–526, 2010.
[2] L. Vivien *et al.*, "42 GHz p.i.n germanium photodetector integrated in a silicon-on-insulator waveguide," *Opt. Express*, vol. 17, no. 8, pp. 6252–6257, Apr. 2009.
[3] M. S. Dahlem *et al.*, "Reconfigurable multi-channel second-order silicon microring-resonator filterbanks for on-chip WDM systems," *Opt. Express*, vol. 19, no. 1, pp. 306–316, Jan. 2011.
[4] S. Manipatruni, L. Chen, and M. Lipson, "Ultra high bandwidth WDM using silicon microring modulators," *Opt. Express*, vol. 18, no. 16, pp. 16 858–16 867, Aug. 2010.
[5] S. Feng *et al.*, "Silicon photonics: from a microresonator perspective," *Laser Photonics Rev.*, vol. 6, no. 2, pp. 145–177, 2012.
[6] A. N. Tait, M. A. Nahmias, B. J. Shastri, and P. R. Prucnal, "Broadcast and weight: An integrated network for scalable photonic spike processing," *J. Lightw. Technol.*, vol. 32, no. 21, pp. 3427–3439, Nov. 2014.
[7] G. Indiveri *et al.*, "Neuromorphic silicon neuron circuits," *Front. Neu-*

[41] Y. Wang